

Synthesis, Biological Activity, and Molecular Modeling Investigation of New Pyrazolo[4,3-*e*]-1,2,4-triazolo[1,5-*c*]pyrimidine Derivatives as Human A₃ Adenosine Receptor Antagonists

Pier Giovanni Baraldi,^{*,†} Barbara Cacciari,[†] Stefano Moro,^{*,‡} Giampiero Spalluto,^{*,§} Giorgia Pastorin,[§] Tatiana Da Ros,[§] Karl-Norbert Klotz,^{||} Katia Varani,[⊥] Stefania Gessi,[⊥] and Pier Andrea Borea[⊥]

Dipartimento di Scienze Farmaceutiche, and Dipartimento di Medicina Clinica e Sperimentale-Sezione di Farmacologia, Università degli Studi di Ferrara, Via Fossato di Mortara 17-19, I-44100 Ferrara, Italy; Dipartimento di Scienze Farmaceutiche, Università degli Studi di Trieste, Piazzale Europa 1, I-34127 Trieste, Italy; Molecular Modeling Section, Dipartimento di Scienze Farmaceutiche, Università di Padova, via Marzolo 5, I-35131 Padova, Italy; and Institut für Pharmakologie, Universität Würzburg, Versbacher Str.9, D-97078 Würzburg, Germany

Received June 21, 2001

A new series of pyrazolotriazolopyrimidines bearing different substitutions on the phenylcarbamoyl moieties at the N5 position, being highly potent and selective human A₃ adenosine receptor antagonists, is described. The compounds represent an extension and an improvement of our previous work on this class of compounds (*J. Med. Chem.* **1999**, *42*, 4473–4478; *J. Med. Chem.* **2000**, *43*, 4768–4780). All the synthesized compounds showed A₃ adenosine receptor affinity in the subnanomolar range and high levels of selectivity in radioligand binding assays at the human A₁, A_{2A}, A_{2B}, and A₃ adenosine receptors. In particular, the effect of the substitution and its position on the phenyl ring have been studied. From binding data, it is evident that the unsubstituted derivatives on the phenyl ring (e.g., compound **59**, hA₃ = 0.16 nM, hA₁/hA₃ = 3713, hA_{2A}/hA₃ = 2381, hA_{2B}/hA₃ = 1388) showed the best profile in terms of affinity and selectivity at the human A₃ adenosine receptors. The introduction of a sulfonic acid moiety at the para position on the phenyl ring was attempted in order to design water soluble derivatives. However, this substitution led to a dramatic decrease of affinity at all four adenosine receptor subtypes. A computer-generated model of the human A₃ receptor was built and analyzed to better interpret these results, demonstrating that steric control, in particular at the para position on the phenyl ring, plays a fundamental role in the receptor interaction. Some of the synthesized compounds proved to be full antagonists in a specific functional model, where the inhibition of cAMP-generation by IB-MECA was measured in membranes of CHO cells stably transfected with the human A₃ receptor with IC₅₀ values in the nanomolar range, with a statistically significant linear relationship with the binding data.

Introduction

Many physiological functions may be regulated by interaction of adenosine with a set of specific receptors, classified as A₁, A_{2A}, A_{2B}, and A₃. For this reason, adenosine receptors could be considered as potential targets in the treatment of different pathophysiological conditions. Adenosine receptor subtypes belong to the family of seven transmembrane domain receptor coupled G proteins and exert their physiological role by activation or inhibition of different second messenger systems. In particular, the modulation of adenylate cyclase activity could be considered to be the prominent signal mediated by these receptors subtypes.^{1,2}

In the last 20 years, intense medicinal chemistry efforts led to the synthesis of a variety of adenosine

receptor agonists and antagonists for the pharmacological characterization of this family of G-protein coupled receptors. Although potent and selective ligands have been identified for the A₁, A_{2A}, and A₃ receptors, there is still a need for such ligands for the A_{2B} subtype.^{1,3}

The A₃ adenosine receptor subtype, recently cloned from different species (e.g., rat, human, dog, sheep),^{4–9} is coupled to the modulation of at least two second messenger systems: inhibition of adenylate cyclase³ and stimulation of phospholipase C¹⁰ and D.¹¹ Activation of A₃ adenosine receptors also causes the release of inflammatory mediators such as histamine from mast cells, in a rat model.¹² In human, A₃ receptors have been found in several organs, such as lung, liver, kidney, and heart, with a lower density in the brain.¹³ This receptor subtype is under examination in relation to its potential therapeutic applications. In particular, antagonists for A₃ receptors seem to be useful for the treatment of inflammation¹⁴ and regulation of cell growth.^{15,16}

In the last 5 years, many efforts have been conducted for searching potent and selective human A₃ adenosine antagonists. In this field many different classes of compounds have been proposed,¹⁷ possessing good affinity (nM range) but without significant selectivity.^{17a,b}

* Corresponding author. Phone +39-(0)532-291293. Fax +39-(0)532-291296. E-mail pgb@dns.unife.it.

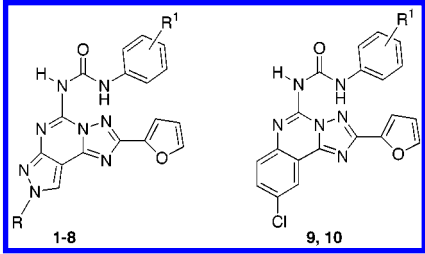
[†] Dipartimento di Scienze Farmaceutiche, Università degli Studi di Ferrara.

[‡] Università di Padova.

[§] Università degli Studi di Trieste.

^{||} Universität Würzburg.

[⊥] Dipartimento di Medicina Clinica e Sperimentale-Sezione di Farmacologia, Università degli Studi di Ferrara.

Table 1. Structures and Binding Affinity at hA₁, hA_{2A}, hA_{2B}, and hA₃ Adenosine Receptors of the Most Interesting Compounds Previously Reported


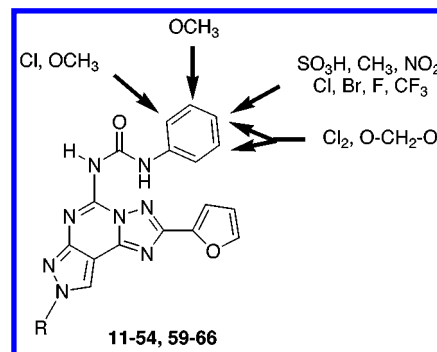
compd	R	R ¹	hA ₁ (K _i , nM) ^a	hA _{2A} (K _i , nM) ^b	hA _{2B} (K _i , nM) ^c	hA ₃ (K _i , nM) ^d	hA ₁ /hA ₃	hA _{2A} /hA ₃	hA _{2B} /hA ₃
1	CH ₃	4-OMe	1097 (928–1297)	1390 (1220–1590)	261 (226–301)	0.20 (0.17–0.24)	5485	6950	1305
2	CH ₃	3-Cl	350 (323–378)	1195 (1024–1396)	205 (157–268)	0.40 (0.24–0.64)	875	2987	512
3	C ₂ H ₅	4-OMe	1026 (785–1341)	1040 (830–1310)	245 (188–320)	0.60 (0.51–0.70)	1710	1733	408
4	C ₂ H ₅	3-Cl	249 (215–289)	180 (160–210)	150 (107–210)	1.60 (1.42–1.79)	155	112	93.7
5	<i>n</i> -C ₃ H ₇	4-OMe	1197 (1027–1396)	140 (120–155)	2056 (1637–2582)	0.80 (0.63–0.1.00)	1496	175	2570
6	<i>n</i> -C ₃ H ₇	3-Cl	30 (23–40)	1220 (880–1682)	57 (50–63)	0.91 (0.85–0.98)	33	1340	62.6
7	<i>n</i> -C ₄ H ₉	4-OMe	296 (269–326)	80 (65–92)	303 (260–352)	0.32 (0.27–0.34)	925	250	946
8	<i>n</i> -C ₄ H ₉	3-Cl	245 (213–281)	95 (70–130)	70 (56–89)	0.60 (0.52–0.68)	408	158	116
9		4-OMe	7.6 (6.5–8.7)	9.4 (8.7–10.2)	22 (19–27)	0.14 (0.08–0.24)	43	50	158
10		3-Cl	8.1 (6.9–9.7)	9.5 (8.7–10.5)	30 (23–40)	0.19 (0.13–0.27)	54	67	157

^a Displacement of specific [³H]DPCPX binding at human A₁ receptors expressed in CHO cells (*n* = 3–6). ^b Displacement of specific [³H]SCH58261 binding at human A_{2A} receptors expressed in CHO cells (*n* = 3–6). ^c Displacement of specific [³H]DPCPX binding at human A_{2B} receptors expressed in HEK-293 cells (*n* = 3–6). ^d Displacement of specific [³]MRE-3008F20 binding at human A₃ receptors expressed in CHO cells (*n* = 3–6). Data are expressed as geometric means, with 95% confidence limits.

Recently, our group proposed a series of pyrazolo-triazolopyrimidines bearing, at the amino group in 5 position, the 3-chlorophenylcarbamoyl or the 4-methoxyphenylcarbamoyl residues, respectively, as highly potent and selective human A₃ adenosine receptor antagonists.^{18,19} (Table 1)

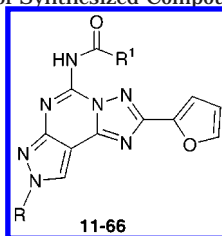
Table 1 briefly summarizes the most interesting compounds (**1–10**) previously synthesized as human A₃ adenosine receptor antagonists.¹⁹ It is clearly evident that the 4-methoxy group on the phenyl ring confers more affinity versus the human A₃ receptors if compared with the 3-chloro substitution. In addition, the optimal affinity and selectivity for the human A₃ adenosine receptors was obtained with the presence of a small alkyl chain at the N⁸ position. In fact, the combination of the 4-methoxyphenylcarbamoyl moiety at the N⁵ position with the methyl group at the N⁸ pyrazole nitrogen resulted in compound (**1**), which shows the best binding profile both in terms of affinity and selectivity (hA₃ = 0.2 nM, hA₁/hA₃ = 5485; hA_{2A}/hA₃ = 6950; hA_{2B}/hA₃ = 1305) ever reported.

Starting from these experimental observations, we decided to investigate the steric and the electronic properties of the substituents on the phenyl ring necessary for the receptor recognition. For this purpose, different groups were introduced at the 4 position on the phenyl ring, and at the same time, small alkyl chains (methyl, ethyl, *n*-propyl, *n*-butyl) were maintained at the N⁸ position. The effect of the position of the substitution (ortho, meta, and para) of the chloro

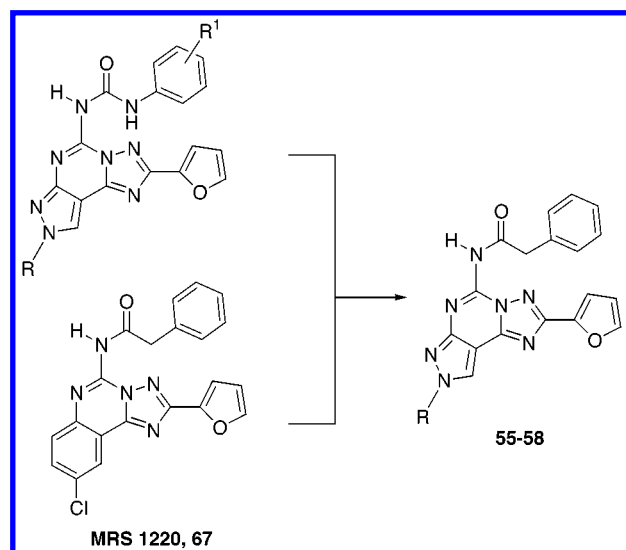
**Figure 1.** General modifications of designed compounds.

or methoxy substituents, introduced in the previous series,^{18,19} has been also evaluated (Figure 1).

As previously reported, we also demonstrated the importance of the pyrazole nitrogen for both affinity and selectivity. In fact, derivatives **9** and **10**, derived from the triazoloquinazoline CGS 15943 substituted at the N5 position with phenyl carbamoyl moieties, showed good affinity for the A₃ adenosine receptor, but a significant loss of selectivity vs other receptor subtypes was observed.¹⁹ With the aim to better investigate all the structural requirements necessary for the human A₃ adenosine receptor interaction, we replaced the arylcarbamoyl function with the phenylacetamyl group characteristic of the nonselective human A₃ antagonist 5-phenylacetamino-9-chloro-2-(2-furyl)[1,2,4]triazolo-[1,5-*c*]quinazoline (MRS1220, **67**), reported by Jacobson and co-workers²⁰ (Figure 2).

Table 2. Structures and Physicochemical Parameters of Synthesized Compounds

compd	R	R ¹	mp (°C)	MW	compd	R	R ¹	mp (°C)	MW
59	CH ₃	Ph-NH	165–167	384.20	33	<i>n</i> -C ₃ H ₇	3,4-Cl ₂ -Ph-NH	208	470.07
63	CH ₃	4-SO ₃ H-Ph-NH	255	450.08	34	<i>n</i> -C ₃ H ₇	3,4-OCH ₂ O-Ph-NH	111–113	446.14
11	CH ₃	3,4-Cl ₂ -Ph-NH	204	442.04	35	<i>n</i> -C ₃ H ₇	4-NO ₂ -Ph-NH	190	447.14
12	CH ₃	3,4-OCH ₂ O-Ph-NH	118–120	418.11	36	<i>n</i> -C ₃ H ₇	4-CH ₃ -Ph-NH	181–184	416.16
13	CH ₃	4-NO ₂ -Ph-NH	180	419.10	37	<i>n</i> -C ₃ H ₇	4-Br-Ph-NH	225	481.31
14	CH ₃	4-CH ₃ -Ph-NH	195–197	388.13	38	<i>n</i> -C ₃ H ₇	4-F-Ph-NH	193	420.40
15	CH ₃	4-Br-Ph-NH	>300	453.26	39	<i>n</i> -C ₃ H ₇	4-CF ₃ -Ph-NH	202	470.41
16	CH ₃	4-F-Ph-NH	>300	392.35	40	<i>n</i> -C ₃ H ₇	2-OMe-Ph-NH	195	432.44
17	CH ₃	4-CF ₃ -Ph-NH	203	442.36	41	<i>n</i> -C ₃ H ₇	3-OMe-Ph-NH	175	432.44
18	CH ₃	2-OMe-Ph-NH	>300	404.39	42	<i>n</i> -C ₃ H ₇	2-Cl-Ph-NH	185	436.86
19	CH ₃	3-OMe-Ph-NH	205	404.39	43	<i>n</i> -C ₃ H ₇	4-Cl-Ph-NH	216	436.86
20	CH ₃	2-Cl-Ph-NH	>300	408.80	62	<i>n</i> -C ₄ H ₉ ^a	Ph-NH	145	416.17
21	CH ₃	4-Cl-Ph-NH	225	408.80	66	<i>n</i> -C ₄ H ₉	4-SO ₃ H-Ph-NH	240–241	496.12
60	C ₂ H ₅ ^a	Ph-NH	180	388.13	44	<i>n</i> -C ₄ H ₉	3,4-Cl ₂ -Ph-NH	205–206	484.09
64	C ₂ H ₅	4-SO ₃ H-Ph-NH	225	468.09	45	<i>n</i> -C ₄ H ₉	3,4-OCH ₂ O-Ph-NH	115–117	460.16
22	C ₂ H ₅	3,4-Cl ₂ -Ph-NH	185–188	456.06	46	<i>n</i> -C ₄ H ₉	4-NO ₂ -Ph-NH	195	461.15
23	C ₂ H ₅	3,4-OCH ₂ O-Ph-NH	124–126	432.12	47	<i>n</i> -C ₄ H ₉	4-CH ₃ -Ph-NH	175–177	430.18
24	C ₂ H ₅	4-NO ₂ -Ph-NH	185	433.12	48	<i>n</i> -C ₄ H ₉	4-Br-Ph-NH	227	495.34
25	C ₂ H ₅	4-CH ₃ -Ph-NH	175–178	402.15	49	<i>n</i> -C ₄ H ₉	4-F-Ph-NH	207	434.43
26	C ₂ H ₅	4-Br-Ph-NH	220	467.28	50	<i>n</i> -C ₄ H ₉	4-CF ₃ -Ph-NH	221	484.44
27	C ₂ H ₅	4-F-Ph-NH	200	406.38	51	<i>n</i> -C ₄ H ₉	2-OMe-Ph-NH	186	446.47
28	C ₂ H ₅	4-CF ₃ -Ph-NH	180	456.39	52	<i>n</i> -C ₄ H ₉	3-OMe-Ph-NH	185	446.47
29	C ₂ H ₅	2-OMe-Ph-NH	128	418.41	53	<i>n</i> -C ₄ H ₉	2-Cl-Ph-NH	185	450.89
30	C ₂ H ₅	3-OMe-Ph-NH	178	418.41	54	<i>n</i> -C ₄ H ₉	4-Cl-Ph-NH	210	450.89
31	C ₂ H ₅	2-Cl-Ph-NH	127	422.83	55	CH ₃	Ph-CH ₂	198–200	373.12
32	C ₂ H ₅	4-Cl-Ph-NH	220	422.83	56	C ₂ H ₅	Ph-CH ₂	106–108	387.14
61	<i>n</i> -C ₃ H ₇ ^a	Ph-NH	155	402.15	57	<i>n</i> -C ₃ H ₇	Ph-CH ₂	101–103	401.16
65	<i>n</i> -C ₃ H ₇	4-SO ₃ H-Ph-NH	235	482.11	58	<i>n</i> -C ₄ H ₉	Ph-CH ₂	101	415.17

^a See Baraldi et al. *J. Med. Chem.* **2001**, *44*, 2735–2742.**Figure 2.** Rational design of hybrid derivatives (**55–58**) between MRS 1220 (**67**) and the pyrazolotriazolopyrimidine series.

Chemistry

Compounds **11–66** (Table 2) were prepared following the general synthetic strategy summarized in Schemes 1 and 3.

The final compounds (**11–54**) were obtained by a coupling reaction of the previously reported derivatives

68–71 with the commercially available isocyanates **72–80**¹⁹ (Scheme 1).

When not commercially available, the isocyanates (**81**, **82**) were prepared by reacting the corresponding substituted anilines with trichloromethylchloroformate, as described in the literature.²¹

The sulfonic acid derivatives **63–66** were prepared starting from the already reported phenyl carbamoyl derivatives **59–62**,²² by reaction with chlorosulfonic acid at 0 °C. Subsequent hydrolysis of the chlorosulfonyl derivative in dioxane (2 mL) and 10% aqueous HCl afforded desired final compounds **63–66**, which were purified by preparative HPLC using a reverse phase column (Scheme 2).

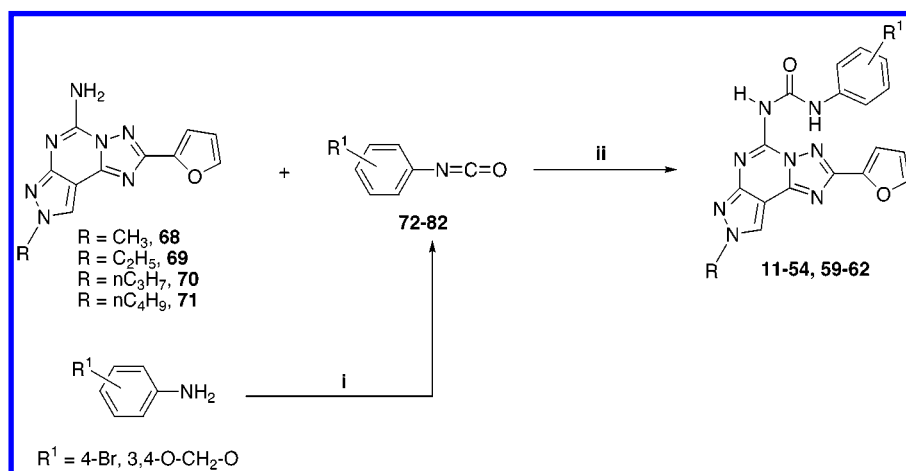
The latest compounds of this series (**55–58**), structurally related to MRS 1220 (**67**), were prepared by acylation with phenylacetyl chloride (1.3 equiv) of the unsubstituted derivatives **68–71** in dry THF at reflux (18 h) in the presence of triethylamine (1.3 equiv) (Scheme 3).

Results and Discussion

Table 3 summarizes the receptor binding affinities of compounds **11–66** determined at the human A₁, A_{2A}, A_{2B}, and A₃ receptors expressed in CHO (A₁, A_{2A}, A₃) and HEK-293 (A_{2B}) cells.

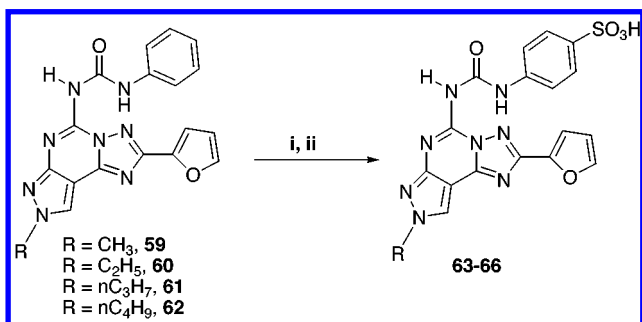
[³H]-1,3-dipropyl-8-cyclopentyl xanthine ([³H]DPC-PX)^{23,24} (A₁ and A_{2B}), [³H]-5-amino-7-(2-phenylethyl)-2-(2-furyl)pyrazolo[4,3-*e*]-1,2,4-triazolo[1,5-*c*]-pyrimidine

Scheme 1



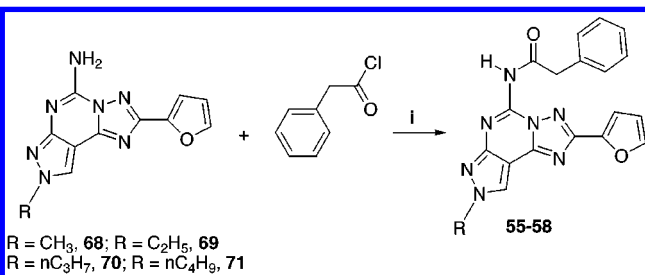
Reagents: (i) ClCOOCCl_3 , dioxane, reflux; (ii) dry THF, reflux, 18 h.

Scheme 2



Reagents: (i) chlorosulfonic acid, 0 °C, 4 h; (ii) dioxane, 10 M HCl, rt, 2 days, then preparative HPLC.

Scheme 3



Reagents: (i) dry THF, Et_3N , reflux, 18 h.

([³H]-SCH 58261) ($\text{A}_{2\text{A}}$),²⁵ and [³H]-5-(4-methoxyphenyl-carbamoyl)amino-8-propyl-2-(2-furyl)pyrazolo[4,3-*e*]-1,2,4-triazolo[1,5-*c*]pyrimidine ([³H]-MRE3008-F20) (A_3)²⁴ have been used as radioligands in binding assays.

All the synthesized compounds showed affinity in the subnanomolar range for the human A₃ adenosine receptors with different degrees of selectivity versus the other receptor subtypes, confirming, as previously observed, that small alkyl substituents at the N⁸ pyrazole nitrogen are indispensable for having good affinity and selectivity at the hA₃ adenosine receptors.^{18,19}

From a preliminary analysis of the data summarized in Table 3, affinities to the hA₃ receptors seem to correlate more with the position of the substituent than with the nature of the substitution on the phenyl ring. From a careful examination of the binding affinities, it appears evident that the most interesting compounds in terms of both affinity and selectivity are the unsub-

stituted derivatives on the phenyl ring, which display a slight improvement of potency and a good retention of selectivity at the human A₃ adenosine receptors also with respect to the previously substituted-phenyl counterparts (see Table 1) (e.g., compound **59**, hA₃ = 0.16 nM, hA₁/hA₃ = 3713, hA_{2A}/hA₃ = 2381, hA_{2B}/hA₃ = 1388 vs compound **1**, hA₃ = 0.20 nM, hA₁/hA₃ = 5485, hA_{2A}/hA₃ = 6950, hA_{2B}/hA₃ = 1305). Accordingly, a careful check of binding data of derivatives bearing a substituent at the para or meta positions on the phenyl ring do not permit us to find any classical QSAR correlations. In particular, we have tried to correlate, without any success, electronic parameters (measured by σ_p or σ_m constants),²⁶ steric properties (calculated by the corresponding molecular volumes),²⁶ and lipophilic (measured by calculated log *P*) descriptors²⁶ with the affinity value at the human A₃ adenosine receptors.

A molecular modeling investigation has been performed to elucidate the hypothetical binding mode of these new A₃ antagonists and, in particular, to better rationalize the correlation between their chemical structures and the corresponding binding results. Unfortunately, little structural information is available concerning the details of ligand/GPCR interactions. However, very recently a 2.8 Å resolution crystal structure of bovine rhodopsin was published.²⁷ Using a homology approach, we have built an improved model of the transmembrane region of the human A₃ receptor, using the crystal structure of the rhodopsin as a template, which can be considered a further refinement in building the hypothetical binding site of the A₃ receptor antagonists already proposed.²⁸ Details of the model building are given in the Experimental Section.

We have selected derivative **59**, corresponding to the unsubstituted derivative on the phenyl ring, as reference ligand in our docking studies. However, the most stable docked conformation is very similar for all the analyzed compounds. As shown in Figure 3, after the Monte Carlo/annealing sampling, we identified the hypothetical binding site of **59** surrounded by TM3, TM5, TM6, and TM7 with the furan ring pointing toward the extracellular environment. Interestingly, a very similar conformation has been already reported for another potent but not selective human A₃ adenosine receptor antagonist as well CGS 15943.²⁸

Table 3. Binding Affinity at hA₁, hA_{2A}, hA_{2B}, and hA₃ Adenosine Receptors of Synthesized Compounds

compd	hA ₁ (<i>K_i</i> , nM) ^a	hA _{2A} (<i>K_i</i> , nM) ^b	hA _{2B} (<i>K_i</i> , nM) ^c	hA ₃ (<i>K_i</i> , nM) ^d	hA ₁ /hA ₃	hA _{2A} /hA ₃	hA _{2B} /hA ₃
59	594 (436–810)	381 (351–415)	222 (181–273)	0.16 (0.13–0.20)	3713	2381	1388
63	>10000 (436–810)	594	>10000	25 (19–34)	>400	24	>400
11	392 (324–475)	143 (114–179)	116 (91–148)	3.4 (3.05–3.78)	115	42	34
12	1015 (885–1163)	680 (552–839)	142 (128–156)	0.24 (0.21–0.28)	4229	2833	592
13	1115 (984–1263)	695 (534–906)	180 (159–204)	0.43 (0.38–0.48)	2593	1616	419
14	731 (601–888)	110 (93–130)	302 (244–373)	0.31 (0.25–0.38)	2358	355	974
15	600 (512–698)	100 (83–120)	181 (152–216)	0.46 (0.39–0.54)	1304	217	393
16	700 (602–814)	120 (103–140)	226 (183–278)	0.34 (0.28–0.41)	2059	353	665
17	750 (654–856)	140 (112–177)	286 (235–347)	0.74 (0.64–0.86)	1014	189	386
18	450 (379–535)	180 (146–220)	223 (187–265)	0.70 (0.59–0.83)	643	257	319
19	500 (406–616)	160 (140–186)	251 (213–296)	0.80 (0.71–0.91)	625	200	313
20	400 (332–479)	200 (174–230)	101 (89–116)	0.91 (0.82–1.01)	440	220	111
21	430 (351–526)	180 (162–200)	128 (115–143)	0.29 (0.23–0.36)	1483	621	441
60	326 (275–386)	40 (33–48)	88 (67–115)	0.18 (0.13–0.23)	1811	222	489
64	>10000	249 (199–311)	>10000	40 (31–50)	>250	6	>250
22	526 (453–609)	352 (300–414)	40 (32–51)	3.0 (2.7–3.4)	175	117	13
23	802 (724–889)	576 (511–648)	48 (37–63)	0.27 (0.22–0.34)	2970	2133	178
24	1134 (967–1329)	614 (490–768)	226 (192–267)	0.65 (0.56–0.75)	1745	945	348
25	262 (248–276)	30 (23–40)	132 (118–146)	0.14 (0.11–0.18)	1871	214	943
26	500 (389–640)	40 (30–54)	296 (261–336)	0.37 (0.29–0.47)	1351	108	800
27	602 (509–712)	60 (48–78)	246 (211–287)	0.86 (0.77–0.97)	700	70	286
28	450 (346–586)	53 (51–55)	235 (178–310)	0.97 (0.86–1.09)	464	57	242
29	300 (216–412)	133 (108–163)	196 (162–237)	0.56 (0.49–0.64)	536	238	350
30	400 (345–465)	140 (114–170)	215 (184–250)	0.86 (0.77–0.96)	465	163	250
31	348 (267–453)	150 (122–187)	97 (67–141)	0.30 (0.23–0.40)	1160	500	323
32	400 (330–486)	160 (134–190)	85 (68–105)	0.20 (0.15–0.28)	2000	800	425
61	176 (150–207)	62 (40–96)	241 (206–282)	0.15 (0.10–0.18)	1173	413	1606
65	>10000	305 (240–388)	>10000	30 (22–41)	>333	10	>333
33	611 (552–676)	401 (362–445)	31 (25–40)	2.5 (2.0–3.1)	244	160	12
34	842 (738–961)	667 (543–820)	53 (40–69)	0.30 (0.22–0.40)	2807	2223	177
35	1214 (1033–1425)	1115 (984–1263)	305 (240–388)	0.81 (0.63–1.04)	1499	1377	377
36	302 (237–384)	12 (8–18)	46 (34–62)	0.40 (0.31–0.50)	755	30	115
37	350 (290–418)	50 (40–62)	150 (124–180)	0.45 (0.37–0.56)	778	111	333
38	376 (294–480)	42 (34–50)	161 (140–186)	0.29 (0.21–0.40)	1297	145	555
39	400 (330–478)	34 (24–48)	136 (115–161)	0.51 (0.42–0.62)	784	67	267
40	250 (180–345)	100 (73–138)	165 (125–218)	0.34 (0.27–0.43)	735	294	485
41	275 (198–382)	113 (96–133)	175 (149–204)	0.40 (0.32–0.50)	688	283	438
42	300 (245–370)	121 (103–142)	61 (49–77)	0.71 (0.61–0.83)	423	170	86

Table 3 (Continued)

compd	hA ₁ (K _i , nM) ^a	hA _{2A} (K _i , nM) ^b	hA _{2B} (K _i , nM) ^c	hA ₃ (K _i , nM) ^d	hA ₁ /hA ₃	hA _{2A} /hA ₃	hA _{2B} /hA ₃
43	325 (265–400)	140 (123–162)	76 (56–103)	0.34 (0.24–0.48)	956	412	224
62	409 (358–468)	148 (102–215)	50 (43–58)	0.21 (0.12–0.37)	1948	705	238
66	>10000	352 (300–414)	>10000	47 (39–55)	>213	7.49	>213
44	708 (598–838)	495 (402–608)	34 (26–45)	3.7 (3.2–4.3)	191	134	9.19
45	410 (314–536)	376 (332–426)	78 (57–105)	0.50 (0.40–0.62)	820	752	156
46	584 (511–667)	503 (442–571)	52 (45–60)	0.55 (0.46–0.64)	1062	915	96
47	281 (210–376)	24 (18–33)	161 (127–203)	0.21 (0.16–0.28)	1338	114	767
48	300 (222–400)	66 (47–93)	121 (88–165)	0.91 (0.82–1.02)	330	73	133
49	318 (253–401)	50 (36–70)	136 (107–172)	0.80 (0.70–0.92)	398	63	170
50	350 (264–463)	31 (25–40)	130 (105–170)	0.72 (0.61–0.84)	486	43	181
51	200 (156–258)	91 (71–111)	125 (116–134)	0.57 (0.46–0.70)	351	160	219
52	248 (184–333)	95 (78–114)	150 (124–180)	0.60 (0.53–0.68)	413	158	250
53	280 (245–319)	100 (83–120)	78 (65–94)	0.86 (0.76–0.98)	326	116	91
54	300 (240–368)	111 (91–137)	87 (76–98)	0.43 (0.37–0.50)	698	258	202
55	702 (624–790)	423 (379–471)	165 (139–156)	0.81 (0.69–0.97)	867	522	204
56	714 (589–866)	335 (289–437)	161 (132–196)	1.03 (0.79–1.34)	693	345	156
57	351 (269–458)	306 (255–366)	143 (118–173)	1.01 (0.65–1.58)	348	303	142
58	602 (525–691)	400 (312–515)	101 (89–116)	1.11 (0.74–1.67)	542	360	91

^a Displacement of specific [³H]DPCPX binding at human A₁ receptors expressed in CHO cells (*n* = 3–6). ^b Displacement of specific [³H]SCH58261 binding at human A_{2A} receptors expressed in HEK-293 cells. ^c Displacement of specific [³H]DPCPX binding at human A_{2B} receptors expressed in HEK-293 cells (*n* = 3–6). ^d Displacement of specific [³H]MRE3008-F20 binding at human A₃ receptors expressed in HEK-293 cells. Data are expressed as geometric means, with 95% confidence limits.

In this model, the lowest energy conformation of **59** presents the carbamoyl moiety in the 5-position of the pyrazolo[4,3-*e*]1,2,4-triazolo[1,5-*c*]pyrimidine structure surrounded by four polar amino acids: Ser242 (TM6), Ser271 (TM7), His274, and Ser275 (TM7). This region seems to be very critical for the recognition of the antagonist structures. According to the Jacobson's site-directed mutagenesis results for the human A_{2A} receptor, the Ser281, corresponding to Ser275 in the A₃ receptors, was found to be crucial for the binding of both agonists and antagonists.²⁹

The strong interactions between the carbamoyl moiety and these polar amino acids orient the carbamoyl phenyl ring in the middle of TM6 and TM7, as clearly indicated in Figure 4. The receptor region around the para position of the phenyl ring is mostly hydrophobic [Val235 (TM6), Leu236 (TM6), and Asn278 (TM7)]. This environment could justify why polar substituents at the para position are not very well tolerated, as in the case of the sulfonic acid group.

In fact, when a sulfonic acid group was introduced at the para position on the phenyl ring, a very interesting group of water-soluble derivatives were obtained, but a significant reduction of affinity for all four adenosine receptor subtypes was observed. In fact, compounds **63**–**66** lost about 150–300-fold of their affinity vs the hA₃ receptor and became almost inactive at the hA₁ and hA_{2B} subtypes (>10 mM). However, these compounds

displayed affinity for the hA_{2A} subtype (250–600 nM) receptors with a consequent decrease of hA_{2A}/hA₃ selectivity, ranging from 6 to 24.

Evaluation of the ligand binding pocket of the receptor reveals that very limited empty space is present between TM6 and TM7, and consequently, steric control seems to be taking place around the para position of the phenyl ring. In fact, substituents larger than fluorine, chlorine, methoxy, or methyl are not well tolerated (see entries **13**, **24**, **35**, **46** for *p*-NO₂, **17**, **28**, **39**, **50** for *p*-CF₃, or **15**, **26**, **37**, **48** for *p*-Br in Table 3). All these substituents induce a decrease of affinity at the human A₃ adenosine receptors of about 2–5-fold with respect to the unsubstituted derivatives (**59**–**62**) or to the previously reported compounds (Table 1), in which an electron donor group is present at the para position (**1**, **3**, **5**, **7**).

The same very rigid steric control is also active when substituents larger than hydrogen are present at the meta position of the phenyl ring. In this case a strong steric repulsion among substituents, at the meta position, and amino acid side chains of TM6 and TM7 could drastically reduce the affinity at the hA₃ receptor. On the contrary, substituents at the ortho position seem to occupy an empty region of the binding cavity. According with this model, in the chloro-substituted series the change of the position (2- or 4-substitution) does not seem to influence affinity at the hA₁, hA_{2A}, and hA_{2B}

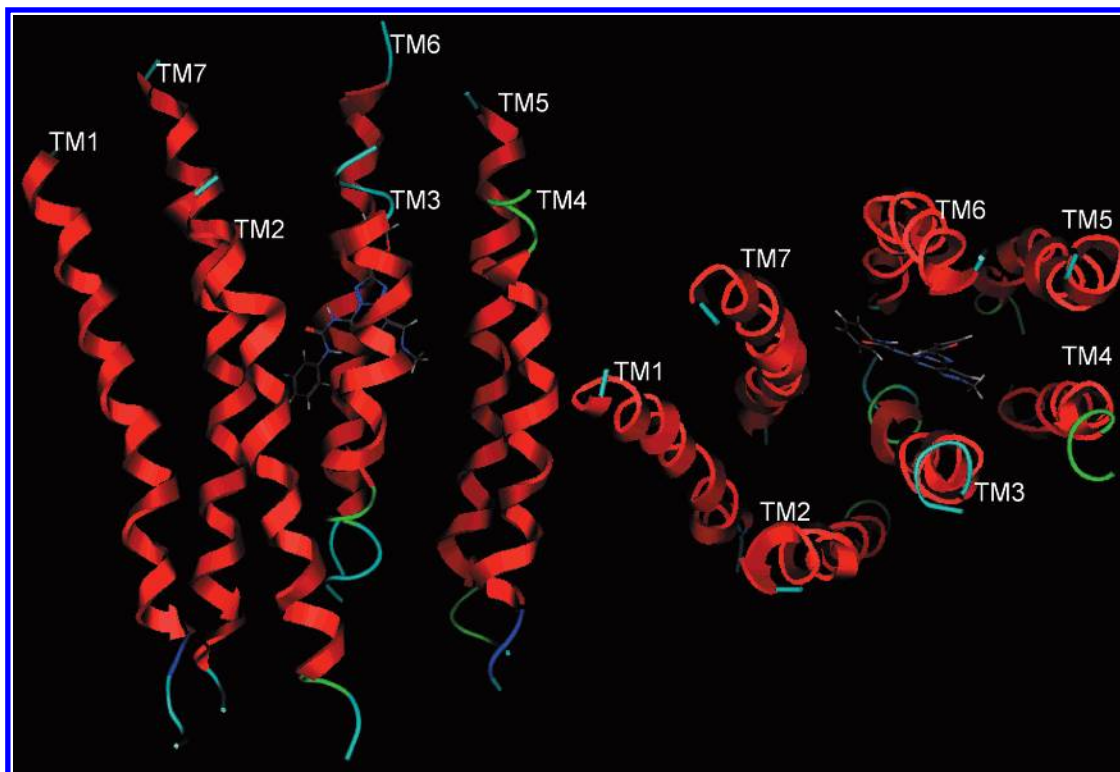


Figure 3. Stereoview of human A₃ transmembrane helical bundle model viewed along the helical axes from the extracellular end (on the right) and perpendicular to the helical axes (on the left). The docked antagonist compound **59** is shown. See Experimental Section for details.

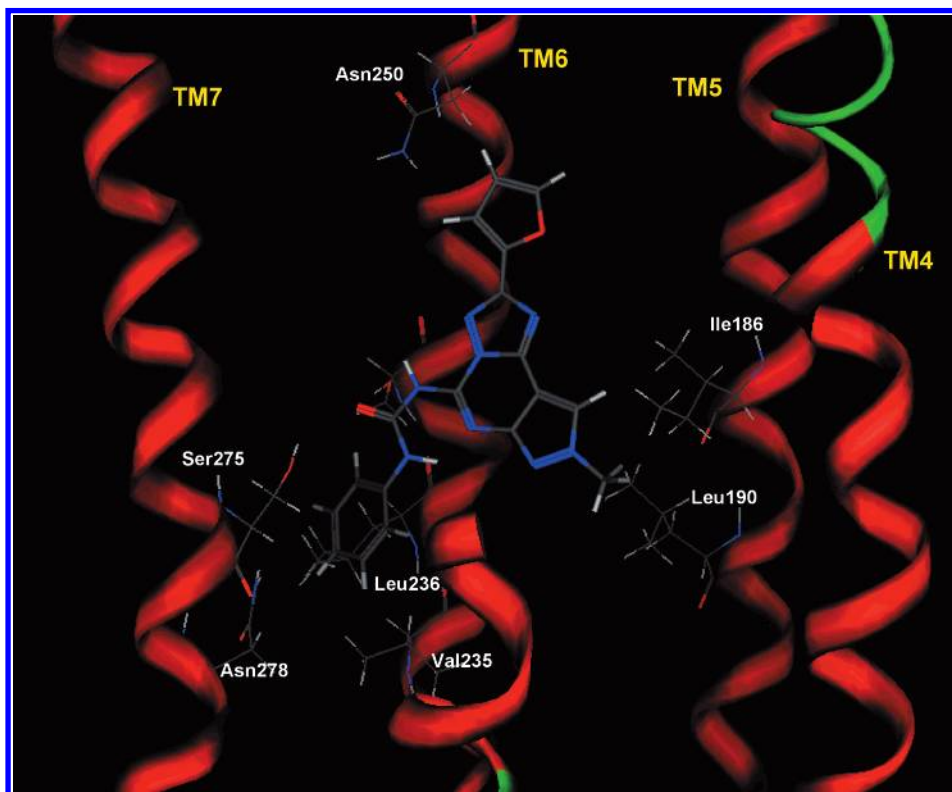


Figure 4. Side view of the A₃-**59** complex model. The side chains of the important residues in proximity (≤ 5 Å) to the docked **59** molecule are highlighted and labeled.

receptors compared to the 3-chloro-substituted compounds **2**, **4**, **6**, **8**, maintaining it in the high nanomolar range (100–500 nM), while significant differences appeared in binding affinity to the hA₃ adenosine receptors. In particular, it is evident that the best position

of substitution is the para position; in fact, a higher affinity in comparison with the previously reported compounds is observed. (e.g., compound **43**, hA₃ = 0.34 nM, hA₁/hA₃ = 956, hA_{2A}/hA₃ = 412, hA_{2B}/hA₃ = 224, vs compound **6**, hA₃ = 0.91 nM, hA₁/hA₃ = 33, hA_{2A}/hA₃

= 1340, hA_{2B}/hA₃ = 63). In contrast, introduction of a chloro atom at the ortho position does not seem to alter significantly the biological profile with respect to the reference compounds, in terms of affinity, but a modest increase of selectivity is obtained (e.g., compound **42**, hA₃ = 0.71 nM, hA₁/hA₃ = 423, hA_{2A}/hA₃ = 170, hA_{2B}/hA₃ = 86, vs compound **6**, hA₃ = 0.91 nM, hA₁/hA₃ = 33, hA_{2A}/hA₃ = 1,340, hA_{2B}/hA₃ = 63). A similar behavior was observed also for the methoxy series, but due to the high levels of affinity, the substitution at the para position was not always the best in terms of potency. In fact, only when the substituent at the N⁸ of the pyrazole nitrogen is methyl or butyl is the 4-methoxy substitution (compounds **1** and **7**, Table 1) optimal in terms of both affinity and selectivity versus the human A₃ adenosine receptors (e.g., compound **18**, hA₃ = 0.7 nM, hA₁/hA₃ = 643, hA_{2A}/hA₃ = 257, hA_{2B}/hA₃ = 319, vs compound **1**, hA₃ = 0.2 nM, hA₁/hA₃ = 5485, hA_{2A}/hA₃ = 6950, hA_{2B}/hA₃ = 1305). If an ethyl or propyl chain is linked to the pyrazole nitrogen, the 2-methoxy substitution gives the best results in terms of affinity when compared to reference compounds (e.g., compound **5**, hA₃ = 0.80 nM, hA₁/hA₃ = 1496, hA_{2A}/hA₃ = 175, hA_{2B}/hA₃ = 2570, vs compound **40**, hA₃ = 0.34 nM, hA₁/hA₃ = 735, hA_{2A}/hA₃ = 294, hA_{2B}/hA₃ = 485).

Another important interaction, probably π - π interaction, is predicted between the CONH₂ group of Asn250 (TM6) and the furan ring of **59**. Also, this asparagine residue, conserved among all adenosine receptor subtypes, was found to be important for ligand binding.³⁰ Moreover, the hydrophobic pocket, delimited by apolar amino acids, such as Leu90 (TM3), Phe182 (TM5), Ile186 (TM5), and Leu190 (TM5), is also present in the binding site model. The amino acids corresponding to Leu90 and Phe182 in the human A_{2A} receptor were found to be essential for the binding of both agonists and antagonists.^{29,30} The methyl group at the N⁸ position of **59** is located within this region of the receptor according to our binding hypothesis. No direct interactions are predicted between the antagonist structure and the two polar amino acids Thr94 (TM3) and Ser97 (TM3). As previously reported, the corresponding two amino acids in the A₁ and A_{2A} receptors, respectively, are important for the coordination of agonists, but not for antagonists.^{29,30}

Another interesting aspect studied in this work is inherent to the evaluation of derivatives bearing at the N⁵ position the phenylacetic chain (**55**–**59**), characteristic of MRS 1220 (**67**). In a previous paper,¹⁹ we have also synthesized two derivatives structurally related to MRS 1220 (**67**)²⁰ by substituting the phenylacetic chain with the urea moieties (derivatives **9**, **10**; Table 1), demonstrating that the phenylcarbamoyl moiety and the pyrazole nitrogens play an important role both for potency and selectivity at the human A₃ adenosine receptor subtypes.

Interestingly, as summarized in Table 3, the synthesized compounds (**55**–**58**) resulted to be about 4–8-fold less potent at the human A₃ adenosine receptors compared to the parent urea derivatives, with a consequent significant loss of selectivity (e.g., compound **55**, hA₃ = 0.81 nM, hA₁/hA₃ = 867, hA_{2A}/hA₃ = 522, hA_{2B}/hA₃ = 204, vs compound **1**, hA₃ = 0.2 nM, hA₁/hA₃ = 5485, hA_{2A}/hA₃ = 6950, hA_{2B}/hA₃ = 1305). Accordingly, our theo-

Table 4. Inhibition of Agonist-Mediated cAMP Production by Compounds with an N⁸-methyl Substituent^a

compd	IC ₅₀ (nM)	compd	IC ₅₀ (nM)
11	26 (15–44)	18	5.6 (3.0–10.8)
12	3.2 (1.8–5.6)	19	7.8 (5.5–10.9)
13	5.5 (4.3–7.0)	20	8.2 (4.4–15.2)
14	4.6 (2.7–7.8)	21	2.4 (1.2–4.9)
15	4.2 (2.7–6.6)	55	6.4 (4.4–9.3)
16	3.0 (2.0–4.3)	59	2.0 (1.4–2.9)
17	6.6 (3.7–11.7)	63	190 (130–279)

^a hA₃ adenosine receptors were stimulated with 100 nM IB-MECA, and the results are shown as IC₅₀ values (nM). Values are the means of at least three experiments and in parentheses the 95% confidence limits are shown.

retical model suggests that the hydrophilic environment created by Ser243 (TM6) and Ser271 (TM7) might be responsible for the fact that NH of the phenylcarbamoyl derivatives is better at accommodating the hypothetical binding site than CH₂ of the phenylacetyl derivatives.

These results seem to suggest, in agreement with previous observations,¹⁹ that the pyrazole nitrogens could modulate the selectivity, while the urea group is able to confer potency versus this receptor subtype.

The synthesized compounds bearing at the N⁸ position the methyl group (compounds **11**–**21**, **55**, **59**, **63**) were also tested for inhibition of cAMP-generation by IB-MECA, in membranes of CHO cells stably transfected with the human A₃ receptor, confirming their antagonistic properties (Table 4).²⁴

This result was in accordance with data from previously synthesized compounds.¹⁹ The potency of the antagonists in the cAMP assay strictly correlated with that observed in binding assays. In fact, comparing the binding data with IC₅₀ values of functional assays resulted in a linear relationship between binding affinity and antagonistic potency, as clearly indicated by the following equation:

$$y = 0.88(\pm 0.03)x + 0.97(\pm 0.02) \quad (r = 0.990)$$

We found another example demonstrating that the inhibition of the human A₃ receptor activity is strictly correlated with the modality of the recognition between antagonist and receptor binding domain.³¹

Conclusions

In conclusion, the present study provides useful information concerning the optimal structural requirements necessary for antagonist recognition of the A₃ adenosine receptor. It demonstrates that the unsubstituted phenylcarbamoyl moiety confers a slightly better affinity for the A₃ adenosine receptor subtype with respect to the para-substituted derivatives (e.g., compound **59**, hA₃ = 0.16 nM, hA₁/hA₃ = 3713, hA_{2A}/hA₃ = 2381, hA_{2B}/hA₃ = 1388, vs compound **1**, hA₃ = 0.20 nM, hA₁/hA₃ = 5485, hA_{2A}/hA₃ = 6950, hA_{2B}/hA₃ = 1305). By the use of molecular modeling studies, it has been demonstrated that the steric factors at the para position on the phenyl ring play a fundamental role for affinity at the human A₃ receptors. In fact, when a sulfonic acid group was introduced in the para position on the phenyl ring, to obtain water-soluble derivatives, a significant reduction of affinity (150–300-fold) at the hA₃ receptor was observed, with a consequent decrease of selectivity versus the other receptor subtypes. In addition, all the

studies performed clearly demonstrated interactions involved in the binding of this class of compounds, such as Ile186 (TM5), Leu190 (TM5), Val235 (TM6), Leu237 (TM6), Ser243 (TM6), Asp250 (TM6), Ser271 (TM7), Ser275 (TM7), and Asp278 (TM7). Thus, this study provides new information about the structural requirements necessary for antagonist–receptor recognition.

Experimental Section

Chemistry. General. Reactions were routinely monitored by thin-layer chromatography (TLC) on silica gel (precoated F₂₅₄ Merck plates) and products visualized with iodine or potassium permanganate solution. Infrared spectra (IR) were measured on a Perkin-Elmer 257 instrument. ¹H NMR were determined in CDCl₃ or DMSO-*d*₆ solutions with a Bruker AC 200 spectrometer, peaks positions are given in parts per million (δ) downfield from tetramethylsilane as internal standard, and *J* values are given in hertz. Light petroleum ether refers to the fractions boiling at 40–60 °C. Melting points were determined on a Buchi-Tottoli instrument and are uncorrected. Chromatographies were performed using Merck 60–200 mesh silica gel. All products reported showed IR and ¹H NMR spectra in agreement with the assigned structures. Organic solutions were dried over anhydrous magnesium sulfate. HPLC separations were conducted with a Waters Delta Prep 3000 A reversed-phase column (30 \times 3 cm, 15 mm). The compounds were eluted with a gradient of 0–60% B in 25 min at a flow rate of 30 mL/min, and the mobile phases were solvent A (10%, v/v, acetonitrile in 0.1% TFA) and solvent B (60%, v/v, acetonitrile in 0.1% TFA). The pure products were converted into the corresponding hydrochloride forms by addition of 0.1 N HCl aqueous solution to the mobile phase containing the pure product. Analytical HPLC analyses were performed on a Bruker liquid chromatography LC 21-C instrument using a Vydac 218 TP 5415 C18 column (250 \times 4 mm, 5 mm particle size) and equipped with a Bruker LC 313 UV variable-wavelength detector. Recording and quantification were accomplished with a chromatographic data processor coupled to an Epson computer system (QX-10). Elemental analyses were performed by the microanalytical laboratory of Dipartimento di Chimica, University of Ferrara, and were within $\pm 0.4\%$ of the theoretical values for C, H, and N.

General Procedures for the Preparation of 5-[(Substituted-phenyl)amino]carbonylamino-8-alkyl-2-(2-furyl)-pyrazolo[4,3-*e*]-1,2,4-triazolo[1,5-*c*]pyrimidine (11–54). Amino compound (**68–71**) (10 mmol) was dissolved in freshly distilled THF (15 mL), and the appropriate isocyanate (**72–82**) (13 mmol) was added. The mixture was refluxed under argon for 18 h. Then the solvent was removed under reduced pressure and the residue was purified by flash chromatography (EtOAc–light petroleum 4:6) to afford the desired compounds **11–54**.

General Procedures for the Preparation of 4-[3-(2-Furan-2-yl-8-alkyl-8*H*-pyrazolo[4,3-*e*][1,2,4]triazolo[1,5-*c*]pyrimidin-5-yl)ureido]benzenesulfonic Acid Derivatives (63–66). To a cooled 0 °C solution of chlorosulfonic acid (2 mL) was added the phenyl urea derivative (**59–62**) (0.35 mmol) in small portions in 20 min. The resulting mixture was stirred at 0 °C for 4 h, then water (15 mL) was added slowly to keep the temperature at 0 °C. The white precipitate (chlorosulfonyl derivative) was filtered and dissolved in dioxane (2 mL) and 10% aqueous HCl, and the solution was stirred at room temperature for 2 days. Then the solvent was removed under reduced pressure, and the residue was purified by preparative HPLC in 25 min at a flow rate of 30 mL/min (reversed phase column; gradient elution 0–60% solvent B), to afford the desired compounds **63–66** as solids.

General Procedures for the Preparation of 5-(Benzyl)carbonylamino-8-alkyl-2-(2-furyl)-pyrazolo[4,3-*e*]-1,2,4-triazolo[1,5-*c*]pyrimidine (55–58). Amino compound (**68–71**) (10 mmol) was dissolved in freshly distilled THF (15 mL), and phenylacetyl chloride (13 mmol) and triethylamine (13 mmol) were added. The mixture was refluxed under argon

for 18 h. Then the solvent was removed under reduced pressure and the residue was dissolved in EtOAc (30 mL) and washed twice with water (15 mL). The organic phase was dried on Na₂SO₄ and concentrated under reduced pressure. The residue was purified by flash chromatography (EtOAc–light petroleum 4:6) to afford the desired compounds as solids.

Biology. CHO Membranes Preparation. The expression of the human A₁, A_{2A}, and A₃ receptors in CHO cells has been previously described.³² The cells were grown adherently and maintained in Dulbecco's modified Eagle's medium with nutrient mixture F12 without nucleosides, containing 10% fetal calf serum, penicillin (100 U/mL), streptomycin (100 μ g/mL), l-glutamine 2 mM, and Geneticin (0.2 mg/mL) at 37 °C in 5% CO₂/95% air. Cells were split two or three times weekly, and then the culture medium was removed for membrane preparations. The cells were washed with phosphate-buffered saline and scraped off flasks in ice-cold hypotonic buffer (5 mM Tris HCl, 2 mM EDTA, pH 7.4). The cell suspension was homogenized with a Polytron and the homogenate was centrifuged for 30 min at 48000*g*. The membrane pellet was resuspended in 50 mM Tris HCl buffer at pH 7.4 for A₁ adenosine receptors; in 50 mM Tris HCl, 10 mM MgCl₂ at pH 7.4 for A_{2A} adenosine receptors; and in 50 mM Tris HCl, 10 mM MgCl₂, 1 mM EDTA at pH 7.4 for A₃ adenosine receptors, and the resuspensions were utilized for binding and adenylate cyclase assays.

Human Cloned A₁, A_{2A}, A_{2B}, and A₃ Adenosine Receptor Binding Assay. Binding of [³H]DPCPX to CHO cells transfected with the human recombinant A₁ adenosine receptor was performed as previously described.²⁴

Displacement experiments were performed for 120 min at 25 °C in 0.20 mL of buffer containing 1 nM [³H]DPCPX, 20 μ L of diluted membranes (50 μ g of protein/assay), and at least six to eight different concentrations of examined compounds. Nonspecific binding was determined in the presence of 10 mM of CHA, and this was always $\leq 10\%$ of the total binding.

Binding of [³H]-SCH58261 to CHO cells transfected with the human recombinant A_{2A} adenosine receptors (50 μ g of protein/assay) was performed according to the method of Varani et al.³³ In competition studies, at least six to eight different concentrations of compounds were used, and nonspecific binding was determined in the presence of 50 mM NECA for an incubation time of 60 min at 25 °C.

Binding of [³H]DPCPX to HEK-293 cells (Receptor Biology Inc., Beltsville, MD) transfected with the human recombinant A_{2B} adenosine receptors was performed as already described.²⁴ In particular, assays were carried out for 60 min at 25 °C in 0.1 mL of 50 mM Tris HCl buffer, 10 mM MgCl₂, 1 mM EDTA, 0.1 mM benzamidine pH 7.4, 2 IU/mL adenosine deaminase containing 40 nM [³H]DPCPX, diluted membranes (20 mg of protein/assay), and at least six to eight different concentration of tested compounds. Nonspecific binding was determined in the presence of 100 mM of NECA and was always $\leq 30\%$ of the total binding.

Binding of [³H]MRE3008-F20 to CHO cells transfected with the human recombinant A₃ adenosine receptors was performed according to the method of Varani et al.²⁴ Competition experiments were carried out in duplicate in a final volume of 250 μ L in test tubes containing 1 nM [³H] MRE3008-F20, 50 mM Tris HCl buffer, 10 mM MgCl₂ (pH 7.4), 100 μ L of diluted membranes (50 μ g protein/assay), and at least six to eight different concentrations of examined ligands. Incubation time was 120 min at 4 °C, according to the results of previous time-course experiments.²⁴ Nonspecific binding was defined as binding in the presence of 1 μ M of MRE3008-F20 and was about 25% of total binding. Bound and free radioactivity were separated by filtering the assay mixture through Whatman GF/B glass-fiber filters using a Micro-Mate 196 cell harvester (Packard Instrument Co.). The filter-bound radioactivity was counted on a Top Count instrument (efficiency 57%) with Micro-Scint 20. The protein concentration was determined according to the Bio-Rad method³⁴ with bovine albumin as reference standard.

Adenylate Cyclase Assay. Membranes were suspended in 0.5 mL of incubation mixture (50 mM Tris HCl, MgCl₂ 10

mM, EDTA 1 mM, pH 7.4) containing GTP 5 μ M, 0.5 mM 4-(3-buthoxy-4-methoxybenzyl)-2-imidazolidinone (Ro 20-1724) as phosphodiesterase inhibitor, and 2.0 IU/mL adenosine deaminase and preincubated for 10 min in a shaking bath at 37 °C. Then IB-MECA or antagonists examined plus ATP (1 mM) and forskolin (10 mM) was added to the mixture and the incubation continued for an additional 10 min. The potencies of antagonists were determined by antagonism of the inhibition of cyclic-AMP production induced by IB-MECA (100 nM). The reaction was terminated by transfer to a boiling water bath. After 2 min at boiling temperature the tubes were cooled to 4 °C and centrifuged at 2000g for 10 min. Supernatants (100 μ L) were used in a protein competition assay for c-AMP carried out essentially according to the method of Varani et al.²⁴

Samples of cyclic AMP standards (0–10 pmol) were added to each test tube containing the incubation buffer (trizma base, 0.1 M; aminophylline, 8.0 mM; 2-mercaptoethanol, 6.0 mM; pH 7.4) and [³H]cyclic AMP in a total volume of 0.5 mL. The binding protein, previously prepared from beef adrenals, was added to the samples previously incubated at 4 °C for 150 min and, after the addition of charcoal, the samples were centrifuged at 2000g for 10 min. The clear supernatant (0.2 mL) was mixed with 4 mL of atomlight in a LS-1800 Beckman scintillation counter.

Computational Approach. All calculations were performed on a Silicon Graphics Octane R12000 workstation.

The human A₃ receptor model was built and optimized using the MOE (2000.02) modeling package³⁵ based on the approach described by Moro et al.³⁶ Briefly, transmembrane domains were identified with the aid of Kyte–Doolittle hydrophobicity and E_{min} surface probability parameters.³⁷ Transmembrane helices were built from the sequences and minimized individually. The minimized helices were then grouped together to form a helical bundle matching the overall characteristics of the recently published crystal structure of bovine rhodopsin (PDB ID: 1F88). The helical bundle was minimized using the Amber94 all-atoms force field,³⁸ until the rms value of the conjugate gradient (CG) was <0.01 kcal/mol/Å. A fixed dielectric constant = 4.0 was used throughout these calculations.

All pyrazolo[4,3-*e*]-1,2,4-triazolo[1,5-*c*]pyrimidine derivatives were fully optimized without geometry constraints using RHF/AM1 semiempirical calculations.³⁹ Vibrational frequency analyses were used to characterize the minimal stationary points (zero imaginary frequencies). The software package Gaussian-98 was utilized for all quantum mechanical calculations.⁴⁰

The ligands were docked into the hypothetical TMs binding site by using the DOCK docking program, part of the MOE suite.³⁵ This program incorporates the use of manual and automatic docking procedures in combination with molecular mechanics within the Simulations module of MOE. The docking method employed enables nonbonded van der Waals and electrostatic interactions to be simultaneously monitored during the docking, and several possible conformations for the ligand were evaluated interactively. "Flexible" ligand docking was then used to define the lowest energy position of each ligand using a Monte Carlo/annealing based automated docking protocol. This uses a random iterative algorithm to sample changes in torsion angles and atomic positions while simultaneously recalculating internal and interaction energies. The automated docking procedure then selected the best structures and subjected the totality of the binding site. During the docking, all torsion angles of the side chains on the ligand were allowed to vary. This docking procedure was followed by another sequence of CG energy minimization to a gradient threshold of < 0.1 kcal/mol/Å. Energy minimization of the complexes was performed using AMBER94 all-atom force field.

The interaction energy values were calculated as follows: $\Delta E_{\text{complex}} = E_{\text{complex}} - (E_{\text{L}} + E_{\text{receptor}})$. These energies are not rigorous thermodynamic quantities but can only be used to compare the relative stabilities of the complexes. Consequently, these interaction energy values cannot be used to calculate binding affinities, since changes in entropy and solvation effects are not taken into account.

Abbreviations: CGS15943, 5-amino-9-chloro-2-(2-furyl)-[1,2,4]triazolo[1,5-*c*]quinazoline; MRS1220, 9-chloro-2-(2-furyl)-[1,2,4]triazolo[1,5-*c*]quinazoline; CHA, N⁶-cyclohexyladenosine; DPCPX, 1,3-dipropyl-8-cyclopentylxanthine; DMSO, dimethyl sulfoxide; THF, tetrahydrofuran; CHO cells, Chinese hamster ovary cells; EDTA, ethylenediaminetetraacetate; SCH58261, 5-amino-2-(2-furyl)-7-(2-phenylethyl)pyrazolo[4,3-*e*]-[1,2,4]triazolo[1,5-*c*]pyrimidine; IB-MECA, 3-iodobenzyl-5'-(N-ethylcarbamoyl)adenosine; NECA, 5'-(N-ethylcarbamoyl)-adenosine; HEK cells, human embryonic kidney cells; MRE3008-F20, 5-[[4-(methoxyphenyl)amino]carbonyl]amino-8-propyl-2-(2-furyl)-pyrazolo[4,3-*e*]-1,2,4-triazolo[1,5-*c*]pyrimidine; GTP, guanosine-5'-triphosphate; cAMP, cyclic adenosine-5'-monophosphate; ATP, adenosine-5'-triphosphate; TLC, thin-layer chromatography; HCl, hydrochloric acid; mp, melting point; EtOAc, ethyl acetate; HPLC, high performance liquid chromatography; IR, infrared spectra; NMR, nuclear magnetic resonance; CDCl₃, deuterated chloroform.

Acknowledgment. We wish to thank Dr. Kenneth A. Jacobson, NIH, Bethesda, MD, for the use of its human A₃ adenosine receptor model in the molecular modeling studies, and Regione Friuli Venezia Giulia (Fondo 2000), for partial financial support.

Supporting Information Available: Experimental details. This material is available free of charge via the Internet at <http://pubs.acs.org>.

References

- Ralevic, V.; Burnstock, G. Receptors for purines and pyrimidines. *Pharmacol. Rev.* **1998**, *50*, 413–492.
- Olah, M. E.; Stiles, G. L. *Annu. Rev. Pharmacol. Toxicol.* Adenosine receptor subtypes: characterization and therapeutic regulation. **1995**, *35*, 581–606.
- Jacobson, K. A.; Suzuki, F. Recent developments in selective agonists and antagonists acting at purine and pyrimidine receptors. *Drug. Dev. Res.* **1996**, *39*, 289–300.
- Meyerhof, W.; Muller-Brechlin, R.; Richter, D. Molecular cloning of a novel putative G-protein coupled receptor expressed during rat spermiogenesis. *FEBS Lett.* **1991**, *284*, 155–160.
- Sajjadi, F. G.; Firestein, G. S. cDNA cloning and sequence analysis of the human A₃ adenosine receptor. *Biochim. Biophys. Acta* **1993**, *1179*, 105–107.
- Salvatore, C. A.; Jacobson, M. A.; Taylor, H. E.; Linden, J.; Johnson, R. G. Molecular cloning and characterization of the human A₃ adenosine receptor. *Proc. Natl. Acad. Sci. U.S.A.* **1993**, *90*, 10365–10369.
- Linden, J. Cloned adenosine A₃ receptors: Pharmacological properties, species differences and receptor functions. *Trends Pharmacol. Sci.* **1994**, *15*, 298–306.
- Zhao, Z. H.; Ravid, S.; Ravid, K. Chromosomal mapping of the mouse A₃ adenosine receptor gene, adora3. *Genomics* **1995**, *30*, 118–119.
- Hill, R. J.; Oleynek, J. J.; Hoth, C. F.; Kiron, M. A.; Weng, W. F.; Wester, R. T.; Tracey, W. R.; Knight, D. R.; Buchholz, R.; Kennedy, S. P. Cloning, expression and pharmacological characterization of rabbit A₁ and A₃ receptors. *J. Pharmacol. Exp. Ther.* **1997**, *280*, 122–128.
- Abbracchio, M. P.; Brambilla, R.; Kim, H. O.; von Lubitz, D. K. J. E.; Jacobson, K. A.; Cattabeni, F. G-protein-dependent activation of phospholipase-C by adenosine A₃ receptor in rat brain. *Mol. Pharmacol.* **1995**, *48*, 1038–1045.
- Ali, H.; Choi, O. H.; Fraundorfer, P. F.; Yamada, K.; Gonzaga, H. M. S.; Beaven, M. A. Sustained activation of phospholipase-D via adenosine A₃ receptors is associated with enhancement of antigen-ionophore-induced and Ca²⁺-ionophore-induced secretion in a rat mast-cell line. *J. Pharmacol. Exp. Ther.* **1996**, *276*, 837–845.
- (a) van Schaick, E. A.; Jacobson, K. A.; Kim, H. O.; IJzerman, A. P.; Danhof, M. Haemodynamic effects and histamine release elicited by the selective adenosine A₃ receptor agonists 2-Cl-IB-MECA in conscious rats. *Eur. J. Pharmacol.* **1996**, *308*, 311–314. (b) Marx, D.; Ezeamuzie, C. I.; Nieber, K.; Szelenyi, I. Therapy of bronchial asthma with adenosine receptor agonists or antagonists. *Drug News Perspect.* **2001**, *14*, 89–100. (c) Meade, C. J.; Mierau, J.; Leon, I.; Ensinger, H. A. In vivo role of the adenosine A₃ receptor-N⁶-2-(4-aminophenyl)ethyladenosine induces bronchospasm in bde rats by a neurally mediated mechanism involving cells resembling mast cells. *J. Pharmacol. Exp. Ther.* **1996**, *279*, 1148–1156. (d) Forsythe, P.; Ennis, M. Adenosine, mast cells and asthma. *Inflamm. Res.* **1999**, *48*, 301–307.

- (13) Linden, J.; Taylor, H. E.; Robeva, A. S.; Tucker, A. L.; Stehle, J. H.; Rivkees, S. A.; Fink, J. S.; Reppert, S. M. Molecular cloning and functional expression of a sheep A₃ adenosine receptor with widespread tissue distribution. *Mol. Pharmacol.* **1993**, *44*, 524–532.
- (14) (a) Ramkumar, V.; Stiles, G. L.; Beaven, M. A.; Ali, H. The A₃ adenosine receptors is the unique adenosine receptor which facilitates release of allergic mediators in mast cells. *J. Biol. Chem.* **1993**, *268*, 16887–16890. (b) Hasko, G.; Nemeth, Z. H.; Vizi, E. S.; Salzman, A. L.; Szabo, C. An agonist of adenosine A₃ receptors decreases interleukin-12 and interferon- γ production and prevents lethality in endotoxemic mice. *Eur. J. Pharmacol.* **1998**, *358*, 261–268.
- (15) Jacobson, K. A.; Moro, S.; Kim, Y. C.; Li, A. H. A₃ Adenosine receptors: protective vs damaging effects identified using novel agonists and antagonists. *Drug Dev. Res.* **1998**, *45*, 113–124.
- (16) (a) Abbracchio, M. P.; Ceruti, S.; Brambilla, R.; Barbieri, D.; Camurri, A.; Franceschi, C.; Giammarioli, A. M.; Jacobson, K. A.; Cattabeni, F.; Malorni, V. Adenosine A₃ receptors and viability of astrocytes. *Drug Dev. Res.* **1998**, *45*, 379–386. (b) Brambilla, R.; Cattabeni, F.; Ceruti, S.; Barbieri, D.; Franceschi, C.; Kim, Y.; Jacobson, K. A.; Klotz, K. N.; Lohse, M. J.; Abbracchio, M. P. Activation of the A₃ adenosine receptor effects cell cycle progression and cell growth. *Naunyn-Schmiedeberg's Arch. Pharmacol.* **2000**, *361*, 225–234.
- (17) (a) Baraldi, P. G.; Cacciari, B.; Romagnoli, R.; Merighi, S.; Varani, K.; Borea, P. A.; Spalluto, G. A₃ Adenosine receptor ligands: history and perspectives. *Med. Res. Rev.* **2000**, *20*, 103–128. (b) Baraldi, P. G.; Cacciari, B.; Romagnoli, R.; Spalluto, G.; Varani, K.; Gessi, S.; Merighi, S.; Borea, P. A. Pyrazolo[4,3-*e*]1,2,4-triazolo[1,5-*c*]pyrimidine derivatives: A new pharmacological tool for the characterization of the human A₃ adenosine receptor. *Drug Dev. Res.* **2001**, *51*, 406–415. (c) van Muijlwijk-Koezen, J.E.; Timmerman, H.; IJzerman, A.P. The adenosine A₃ receptor and its ligands. *Progress in Med. Chem.* **2001**, *38*, 61–113.
- (18) Baraldi, P. G.; Cacciari, B.; Romagnoli, R.; Spalluto, G.; Klotz, K.-N.; Leung, E.; Varani, K.; Gessi, S.; Merighi, S.; Borea, P. A. Pyrazolo[4,3-*e*]1,2,4-triazolo[1,5-*c*]pyrimidine derivatives as highly potent and selective human A₃ adenosine receptor antagonists. *J. Med. Chem.* **1999**, *42*, 4473–4478.
- (19) Baraldi, P. G.; Cacciari, B.; Romagnoli, R.; Spalluto, G.; Moro, S.; Klotz, K. N.; Leung, E.; Varani, K.; Gessi, S.; Merighi, S.; Borea, P. A. Pyrazolo[4,3-*e*]1,2,4-triazolo[1,5-*c*]pyrimidine derivatives as highly potent and selective human A₃ adenosine receptor antagonists: Influence of the chain at N⁸ pyrazole nitrogen. *J. Med. Chem.* **2000**, *43*, 4768–4780.
- (20) (a) Kim, Y. C.; Ji, X. D.; Jacobson, K. A. Derivatives of the triazoloquinazoline adenosine antagonist (CGS15943) are selective for the human A₃ receptor subtype. *J. Med. Chem.* **1996**, *39*, 4142–4148. (b) Kim, Y. C.; de Zwart, M.; Chang, L.; Moro, S.; Jacobien, K.; Frijtag, D. K.; Melman, N.; IJzerman, A. P.; Jacobson, K. A. Derivatives of the triazoloquinazoline adenosine antagonist (CGS15943) having high potency at the human A_{2B} and A₃ receptor subtypes. *J. Med. Chem.* **1998**, *41*, 2835–2845.
- (21) Kurita, K.; Iwakura, Y. Trichloromethyl-Chloroformate as a phosgene equivalent: 3-isocyanatopropanoyl chloride. *Org. Synth.* **1988**, *6*, 715–718.
- (22) Baraldi, P. G.; Cacciari, B.; Romagnoli, R.; Moro, S.; Ji, X.-D.; Jacobson, K. A.; Gessi, S.; Borea, P. A.; Spalluto, G. Fluorosulfonyl- and bis-(β -chloroethyl)amino-phenyl functionalized pyrazolo[4,3-*e*]1,2,4-triazolo[1,5-*c*]pyrimidine derivatives as irreversible antagonists at the human A₃ adenosine receptor: molecular modeling studies. *J. Med. Chem.* **2001**, *44*, 2735–2742.
- (23) Lohse, M. J.; Klotz, K.-N.; Lindernborn-Fotinos, J.; Reddington, M.; Schwabe, U.; Olsson, R. A. 8-Cyclopentyl 1–3dipropylxanthine DPCPX a selective high affinity antagonist radioligand for A₁ adenosine receptors. *Naunyn-Schmiedeberg's Arch. Pharmacol.* **1987**, *336*, 204–210.
- (24) Varani, K.; Merighi, S.; Gessi, S.; Klotz, K. N.; Leung, E.; Baraldi, P. G.; Cacciari, B.; Spalluto, G.; Borea, P. A. [³H]MRE3008-F20: A novel antagonist radioligand for the pharmacological and biochemical characterization of human A₃ adenosine receptors. *Mol. Pharmacol.* **2000**, *57*, 968–975.
- (25) Zocchi, C.; Ongini, E.; Ferrara, S.; Baraldi, P. G.; Dionisotti, S. Binding of the radioligand [³H]-SCH58261, a new nonxanthine A_{2A} adenosine receptor antagonist, to rat striatal membranes. *Br. J. Pharmacol.* **1996**, *117*, 1381–1386.
- (26) Hansch, C.; Leo, A.; Hoekman, D. In *Exploring QSAR: Hydrophobic, Electronic, and Steric Constants*; American Chemical Society: Washington, DC, 1995.
- (27) Palczewski, K.; Kumasaka, T.; Hori, T.; Behnke, C. A.; Motoshima, H.; Fox, B. A.; Trong, I. L.; Teller, D. C.; Okada, T.; Stenkamp, R. E.; Yamamoto, M.; Miyano, M. Crystal structure of rhodopsin: A G protein-coupled receptor. *Science* **2000**, *289*, 739–745.
- (28) Moro, S.; Li, A. H.; Jacobson, K. A. Molecular modeling studies of human A₃ adenosine antagonists: structural homology and receptor docking. *J. Chem. Inf. Comput. Sci.* **1998**, *38*, 1239–1248.
- (29) Jiang, Q.; van Rhee, A. M.; Kim, J.; Yehle, S.; Wess, J.; Jacobson, K. A. Hydrophilic side chains in the third and seventh transmembrane helical domains of human A_{2A} adenosine receptors are required for ligand recognition. *Mol. Pharmacol.* **1996**, *50*, 512–521.
- (30) Kim, J.; Wess, J.; van Rhee, A. M.; Shöneberg, T.; Jacobson, K. A. Site-directed mutagenesis identifies residues involved in ligand recognition in the human A_{2A} adenosine receptor. *J. Biol. Chem.* **1995**, *270*, 13987–13997.
- (31) Kenakin, T. P. In *Pharmacologic Analysis of Drug-Receptor Interaction*; Raven Press: New York, 1987.
- (32) Klotz, K. N.; Hessling, J.; Hegler, J.; Owman, C.; Kull, B.; Fredholm, B. B.; Lohse, M. J. Comparative pharmacology of human adenosine receptor subtypes—Characterization of stably transfected receptors in CHO cells. *Naunyn-Schmiedeberg's Arch. Pharmacol.* **1998**, *357*, 1–9.
- (33) Varani, K.; Gessi, S.; Dionisotti, S.; Ongini, E.; Borea, P. A. [³H]-SCH 58261 Labeling of functional A_{2A} adenosine receptors in human neutrophil membranes. *Br. J. Pharmacol.* **1998**, *123*, 1723–1731.
- (34) Bradford, M. M. A rapid sensitive method for the quantification of microgram quantities of protein utilizing the principle of protein dye-binding. *Anal. Biochem.* **1976**, *72*, 248–254.
- (35) Molecular Operating Environment (MOE 2000.02), Chemical Computing Group, Inc., 1255 University St., Suite 1600, Montreal, Quebec, Canada, H3B 3X3.
- (36) Moro, S.; Guo, D.; Camaioni, E.; Boyer, J. L.; Harden, K. T.; Jacobson, K. A. Human P2Y₁ receptor: Molecular modeling and site-directed mutagenesis as tools to identify agonist and antagonist recognition sites. *J. Med. Chem.* **1998**, *41*, 1456–1466.
- (37) Kyte, J.; Doolittle, R. F. A simple method for displaying the hydrophobic character of a protein. *J. Mol. Biol.* **1982**, *157*, 105–132.
- (38) Weiner, S. J.; Kollman, P. A.; Nguyen, D. T.; Case, D. A. An all-atom force field for simulation of protein and nucleic acids. *J. Comput. Chem.* **1986**, *7*, 230–252.
- (39) Dewar, M. J. S. E.; Zoebisch, G.; Healy, E. F. AM1: A New General Purpose Quantum Mechanical Molecular Model. *J. Am. Chem. Soc.* **1985**, *107*, 3902–3909.
- (40) Frisch, M.; Trucks, G. W.; Schlegel, H.; Scuseria, G.; Robb, M.; Cheeseman, J.; Zakrzewski, V.; Montgomery, J.; Stratmann, R. E.; Burant, J. C.; Dapprich, S.; Millam, J.; Daniels, A.; Kudin, K.; Strain, M.; Farkas, O.; Tomasi, J.; Barone, V.; Cossi, M.; Cammi, R.; Mennucci, B.; Pomelli, C.; Adamo, C.; Clifford, S.; Ochterski, J.; Petersson, G. A.; Ayala, P. Y.; Cui, Q.; Morokuma, K.; Malick, D. K.; Rabuck, A. D.; Raghavachari, K.; Foresman, J. B.; Cioslowski, J.; Ortiz, J. V.; Stefanov, B. B.; Liu, G.; Liashenko, A.; Piskorz, P.; Komaromi, I.; Gomperts, R.; Martin, R. L.; Fox, D. J.; Keith, T.; Al-Laham, M. A.; Peng, C. Y.; Nanayakkara, A.; Gonzalez, C.; Challacombe, M.; Gill, P. M. W.; Johnson, B. G.; Chen, W.; Wong, M. W.; Andres, J. L.; Head-Gordon, M.; Replogle, E. S.; Pople, J. A., Gaussian 98 (revision A.6), 1998, Gaussian, Inc, Pittsburgh, PA.

JM0109614